

## MIT Open Access Articles

*Evaluation and prediction of 17th Street Canal I-wall stability using numerical limit analyses*

The MIT Faculty has made this article openly available. **Please share** how this access benefits you. Your story matters.

**Citation:** Yuan, Yixing and Andrew J. Whittle. "Evaluation and prediction of 17th Street Canal I-wall stability using numerical limit analyses." *Journal of Geotechnical and Geoenvironmental Engineering* (June 2013), Vol. 139, No. 6, pp. 841-852.

**Publisher:** American Society of Civil Engineers

**Persistent URL:** <http://hdl.handle.net/1721.1/67022>

**Version:** Author's final manuscript: final author's manuscript post peer review, without publisher's formatting or copy editing

**Terms of use:** Creative Commons Attribution-Noncommercial-Share Alike 3.0



# EVALUATION AND PREDICTION OF 17<sup>TH</sup> STREET CANAL I-WALL STABILITY USING NUMERICAL LIMIT ANALYSES

by

Yixing Yuan<sup>1</sup> & Andrew J. Whittle<sup>2</sup>, M.ASCE

## ABSTRACT

Numerical limit analyses have been used to evaluate the stability of the 17<sup>th</sup> Street Canal I-wall levee during Hurricane Katrina. The potential formation of a water-filled gap along the canal-side soil-wall interface at failure is included in both the lower and upper bound formulations. The analyses replicate published 2D cross-sections and soil properties developed in forensic investigations carried out by the Interagency Performance Evaluation Task Force (IPET), and by the Independent Levee Investigation Team (ILIT). The current results provide an independent basis for understanding and evaluating the proposed failure mechanisms, and demonstrate that a water-filled gap is a necessary condition for the critical I-wall failure mechanism. Further limit analyses calculations produce credible estimates of the surge elevation that caused failure of the 17<sup>th</sup> Street Canal I-wall as well as predictions of a consistent failure mechanism. The numerical limit analyses show clearly how differences in the stability of the I-wall are linked to different interpretations of the stratigraphy and undrained shear strengths by IPET and ILIT. The analyses also show that effects of a thin layer of weak organic clay as postulated by ILIT are not necessary to explain the I-wall failure.

**KEYWORDS:** Upper and lower bound limits, undrained stability, walls, clays, limit equilibrium, lateral loading

---

<sup>1</sup> Graduate Research Assistant, Massachusetts Institute of Technology, Cambridge, MA 02139

<sup>2</sup> Professor of Civil & Environmental Engineering, Massachusetts Institute of Technology, Cambridge, MA.

## INTRODUCTION

The premature breach of the I-wall on the east bank of the 17<sup>th</sup> Street drainage canal in New Orleans was one of most catastrophic events that occurred during Hurricane Katrina. It has attracted particular attention in the geotechnical community, due to design limitations of I-wall levee systems used for hurricane flood protection.

Two major forensic investigations have been carried out: 1) the Interagency Performance Evaluation Task Force (IPET, 2007; Duncan et al., 2008) and 2) the Independent Levee Investigation Team (ILIT, 2006; Seed et al., 2008c). Each team developed 2D cross-sections of I-wall levee at the breach location as shown in Figure 1, based on independent interpretations of 1) the levee geometry, stratigraphy and soil properties including unit weight and shear strength (using data from original design and post-failure investigations); and 2) storm surge data interpreted from a single hydrograph and witness observations. Both teams used similar approaches to analyze the levee performance under the elevated storm surge using non-linear displacement-based finite element methods (FEM)<sup>3</sup> as well as conventional limit equilibrium methods (LEM)<sup>4</sup>. Both investigation teams found that the 17<sup>th</sup> Street Canal breach occurred at surge elevation well below the top of the levee I-wall, and therefore was most likely caused by instability due to undrained failure within the underlying cohesive soils. One key finding favored by both groups is that a water-filled gap formed along the canal-side of the levee I-wall such that hydrostatic pressures extend down to the tip of the wall. This fact significantly increases the driving force due to the storm surge. This loading condition was not considered in the original design, but is consistent with observed behavior in physical model tests commissioned as part of the IPET investigations (Sasanakul et al., 2008).

Both IPET and ILIT studies assume that the water-filled gap develops during the course of the storm and attempt to model this behavior using finite element analyses. This is a difficult process and is only accomplished through an iterative procedure that involves: 1) detection of tensile stress conditions at the soil-wall interface elements (along the canal-side of the wall); 2) manually creating separation once tensile stress occur; and 3) applying hydraulic pressure on both sides of the “created” gap. Levee stability at each storm surge elevation is then evaluated

---

<sup>3</sup> PLAXIS (Brinkgreve et al, 2007) was used by both groups

<sup>4</sup> IPET used UTEXAS (Wright, 1999) and ILIT chose SLOPE/W (Krahn, 2004)

through a ‘c-phi’ reduction approach (Brinkgreve & Bakker, 1991), such that the influence of the water-filled gap is only taken into account once the surge rises above a critical elevation. Limit equilibrium methods are not able to track the gap opening and hence, stability analyses are performed for two limiting cases: 1) with a fully developed gap, and 2) with no gap. For the former case, a hydrostatic pressure is applied to the I-wall from the storm surge elevation to the toe of the wall. None of these analyses demonstrate that the probable water-filled gap is a necessary condition for the most critical failure mechanism.

Apart from issues relating to the existence and influence of the water-filled gap, there are several other discrepancies between IPET and ILIT analyses that affect the calculated stability and related failure mechanism. These differences are related to the subsurface stratigraphy and shear strength distribution (particularly at points beyond the levee toe). The ILIT team (Seed et al., 2008c) also claims that the presence of a thin stratum of very sensitive organic silty-clay significantly reduces the I-wall stability and leads to a different failure mechanism from that reported by IPET (Fig. 1a, b).

The current paper applies techniques of numerical limit analyses as an independent method of evaluating stability for the critical section of the 17<sup>th</sup> Street Canal levee. The numerical limit analyses assume rigid plastic material behavior (i.e., they use identical shear strength parameters to LEM, but avoid complexities associated with FE stability analyses ), and provide lower and upper bounds on the critical loading condition. The current study adapts upper and lower bound formulations presented by Sloan and Kleeman (1995) and Sloan (1988a). Solutions are achieved through linear programming methods that eliminate the need for user-defined search algorithms. The method uses finite element discretization and interpolation of field variables for handling complex geometry and boundary conditions. Similar numerical limit analyses method have been successfully applied for calculations of undrained bearing capacity of footings under combined loading and for basal stability of braced excavations in clay (Ukritchon et al., 1998, 2003, respectively). In the following, the framework of the method is briefly summarized, emphasizing the implementation of techniques that allow for the possible occurrence of a water-filled gap. The methods have been applied to the 17<sup>th</sup> Street Canal analyses based on the published IPET and ILIT models. The results provide an independent basis for understanding and resolving discrepancies between IPET and ILIT studies.

## NUMERICAL LIMIT ANALYSES

Figure 2 shows a schematic summary of the plane-strain numerical limit analyses used for evaluating I-wall levee stability. In the lower bound formulation, the soil mass is discretized into three-noded triangular elements with linear interpolation of stress components  $(\sigma_x, \sigma_y, \tau_{xy})$  over each element (Fig. 2a, b). In contrast to conventional displacement-based finite element methods, the nodes are unique to each element such that stress discontinuities are allowed along shared edges between the elements. The levee wall is modeled using two-noded beam elements connected by one-node zero-dimension joint elements, where beam nodes are unique to each element and each node has two unknown forces,  $F_x$  and  $F_y$ , and one moment  $F_z$  (Fig. 2c). This formulation allows beam elements to carry linearly-varying external tractions, (e.g., the storm-induced hydraulic pressure on the wall), and the soil-structure interaction can be readily modeled by discontinuities between soil and attached beam element as shown in Figure 2d.

The lower bound solution provides a statically admissible stress field that is subjected to constraints of equilibrium (within soil, stress discontinuities, beam and soil-structure interfaces), yield criteria (for soil and beam respectively) and stress boundary conditions. Ukritchon et al. (1998, 2003) give full details of these constraints, which are presented in the form of equalities and inequalities, and assembled in the framework of a linear programming problem. For the undrained levee stability, the driving force attributed to the failure is the storm-induced hydraulic pressure applied on both the wall and the canal bed. The objective function of the lower bound formulation is to maximize the resultant driving force that links the statically admissible stress field through equilibrium and boundary conditions. The resulting linear programming problem is solved by using the active set algorithm after Sloan (1988b).

The same type of soil and structure discretization is utilized in the upper bound formulation (Fig. 2b). The unknown velocity field  $(u, v)$  is assumed to vary linearly within each soil element and velocity discontinuities are allowed along shared edges due to the fact that each element has unique nodes. Each beam element has two linearly-interpolated velocity components  $(u, v)$ , while an additional degree of freedom, angular velocity  $w$ , is assigned to joint elements to enable the formation of plastic hinges along the beam (Fig. 2c). One big advantage of the formulation is that discontinuities can be used for modeling the interface behavior between the wall and soil, allowing slip and/or separation to occur (Fig. 2d).

In the upper bound solution, a kinematically admissible velocity field must satisfy compatibility, velocity boundary conditions and associated flow rules. An upper bound on the critical load is obtained by equating the external rate of work  $W_{ext}$  to the internal power dissipation  $W_{int}$  expended in the kinematically admissible velocity field. The details of the upper bound formulation are referred to in Ukritchon et al. (1998, 2003).

The external rate of work in the current analyses is due to 1) the hydraulic pressure applied on the canal bed, levee slopes and I-wall, and 2) the gravity force of the soil mass:

$$W_{ext} = W_{hyd} + W_g \quad (1)$$

The internal power dissipation is computed from 1) plastic deformation within soil elements, 2) tangential slip along velocity discontinuities and soil-structure interfaces, and 3) hinge failure in beam elements:

$$W_{int} = W_{ele} + W_{dis} + W_{bm} \quad (2)$$

The objective function of the upper bound formulation seeks to minimize the collapse load, i.e., hydraulic pressure by  $Min\{W_{hyd}\}$ . The resulting linear programming problem is solved using an active set algorithm (Sloan, 1988b).

## IMPLEMENTATION OF WATER-FILLED GAP

When calculating the active earth pressure in a dry clay (no free water around), conventional soil mechanics teaches that a separation can occur between soil and structure if no tensile stress is allowed across the interface (e.g., Lambe & Whitman, 1969; Bolton & Powrie, 1987). This is referred to as a tension gap. It can be modeled in stability analyses by imposing a tension-cut-off in the yield criterion for interfaces. If the gap opens beneath a free water field, water may flow into the gap and build up hydraulic pressure on both sides of the interface. Subsequently, this gap will open further under the induced pressure.

For the purpose of stability analyses based on rigid perfect plastic material behavior, the opening of a water-filled gap is similar to the tension gap, and can be approximated through a plastic deformation along the soil-structure interface. The resistance to the gap formation is controlled by the yield criterion of the interface while its development is governed by the associated flow rule. This approach can answer questions about whether the gap will participate in the failure mechanism and how it influences the failure mechanism without considering the complex gap formation process itself.

### *Lower Bound Formulation*

The tension gap in the undrained lower bound analyses assumes no tension can be sustained across the interface (Fig. 3a). This is accomplished by adding a tension-cut-off to the yield criterion as shown in Figure 3c (Tresca criterion of undrained clay is assumed for describing the strength of a rough soil-structure interface) . It implies the normal traction  $\sigma_n$  at the interface must be no less than hydrostatic water pressure  $p_w$  in a potential water-filled gap (Fig. 3b). The yield criterion is modified such that the cut-off value  $p_w$  is calculated for a specified surge elevation. Figure 3d shows the modified criterion accounting for water-filled gap that is composed of

- Tresca yield criterion:  $|\tau| \leq s_u$
- “Hydraulic pressure” cut-off criterion:  $\sigma_n \geq p_w$

where  $\tau$  and  $\sigma_n$  are the shear stress and the total lateral earth pressure along the interface, respectively;  $s_u$  represents the undrained shear strength of clay.

The lower bound formulation with a potential water-filled gap states that all points along the waterside soil-wall interfaces must satisfy the modified yield criterion. By examining the statically admissible stress field, this approach provides a first estimate on the extent of gap opening at the failure state, (i.e., fully developed, partially developed, or non-existent). The effects of the water-filled gap on the levee I-wall stability can be studied through comparisons of factor of safety (FS) in lower bound analyses with and without the proposed gap model.

### *Upper Bound Formulation*

Ukritchon et al. (1998) introduced an inequality constraint of the flow rule for soil-structure interfaces in order to model the separation across the tension gap:

$$\Delta u_n \leq 0 \quad (3)$$

where  $\Delta u_n$  is the normal velocity jump across the interface, and  $\Delta u_n < 0$  indicates separation (i.e., follows the convention that compression is positive). Figure 3c illustrates that the plastic flow upon this constraint is associated with the tension-cut-off criterion and therefore remains kinematically admissible. Figure 3d shows that the flow corresponding to the previously

introduced “hydrostatic water pressure” cut-off criterion also satisfies the same constraint, and therefore Eq. (3) can be readily applied for modeling the separation of a water-filled gap.

As the tension gap occurs under zero normal stress across interface, there is no external work due to this gap opening. However, once water enters the gap, the induced hydraulic pressure will do additional work that extends the gap. The following paragraphs present a strategy to account for this characteristic in the formation of the water-filled gap.

Considering that water will do work on both sides of the gap during separation, hydrostatic pressure  $p_w$  is directly placed on surfaces of both levee soil and the I-wall over the full depth of the canal-side soil-wall interface, (i.e. from the top of levee crest to the toe of the I-wall). As shown in Eq. (4) and (5), an additional external rate of work  $W_{gap}$ , done by  $p_w$  on the potential separation motion expressed in terms of the normal velocity jump  $\Delta u_n$  will appear in the external rate of work. The negative sign in front of the velocity jump ensures a positive  $W_{gap}$  as gap opening. The objective function now becomes  $Min\{W_{hyd} + W_{gap}\}$ .

$$W_{gap} = \int_{L_{gap}} p_w (-\Delta u_n) dt \quad (4)$$

$$W_{ext} = W_{hyd} + W_g + W_{gap} \quad (5)$$

Unlike the reported LEM analyses (ILIT, 2006; IPET, 2007), the numerical limit analyses do not predefine the occurrence of a water-filled gap, but only introduce the possibility. The upper bound velocity field is eventually obtained through an optimization approach (linear programming), and in principle can generate three possible states of the water-filled gap at failure:

- 1) There is no gap, i.e., the  $\Delta u_n = 0$  along the full depth of the soil-wall interface;
- 2) There is a fully-developed water-filled gap, i.e.,  $\Delta u_n < 0$  along the full depth of the soil-wall interface;
- 3) A partial depth water-filled gap appears in the final state.

Although there are multiple possibilities, when later applying this gap model in the 17<sup>th</sup> Street Canal levee stability analyses the results show that a full depth gap occurred at each storm surge.

## EVALUATION OF THE IPET ANALYSES



Numerical limit analyses have been applied to evaluate the 17<sup>th</sup> Street Canal I-wall and levee stability based on the IPET model (IPET, 2007). The cross-section of the IPET model was shown in Figure 1a, with unit weights of the key strata listed in Table 1. The underlying sand layer is neglected in the current analyses, as it has no effect on the current stability calculations. Figure 4a shows the finite-element mesh used for both upper and lower bound limit analyses. The mesh is developed using the FEM generator implemented in the Plaxis<sup>TM</sup> program (Brinkgreve, 2007) and is subsequently modified to endow each triangular element with three unique nodes.

Ladd (2009) has pointed out some key limitations of the IPET model stratigraphy (which makes the unrealistic assumption that the top surface of the lacustrine clay is horizontal), and errors in the total unit weights reported for the lacustrine clay. The current analyses do not address these issues but simply reproduce the published IPET model geometry and soil properties.

The undrained shear strength parameters for each layer are carefully interpreted from the IPET report (2007) and are consistent with values used by IPET for both FEM and LEM analyses. Figure 4c summarizes the strength profiles at several sections of interest. It should be noted that the lacustrine clay is assumed to be normally consolidated throughout the stratum such that the shear strength increases linearly with the same rate (11psf/ft) with depth.

The factor of safety for levee stability follows the conventional definition used in slope stability calculations,  $FS = s_u / \tau_m$ , where  $s_u$  and  $\tau_m$  are the undrained shear strength and the mobilized shear stress, respectively. In the lower and upper bound limit analyses, FS is obtained through an iterative strength-reduction procedure (similar to the c-phi reduction in FEM analyses), i.e., the undrained shear strength of the soil mass is gradually reduced for each trial FS until the hydraulic pressure calculated at a given storm surge elevation is equal to the critical loading.

Figure 5 shows the factor of safety computed by the numerical limit analyses with surge elevations ranging from El. 0ft to El. +10ft for cases: with and without the proposed soil-wall gap model. In each case the limit analyses are able to bound FS within  $\pm 5\text{-}8\%$ . The results of the current limit analyses predict failure at a storm surge elevation, El. +8.50 $\pm$ 1.0ft for the case with a water-filled gap.

The upper bound FS values are in reasonable agreement with limit equilibrium analyses, LEM, reported by IPET (Duncan et al., 2008) where there is no gap between wall and soil and for a second case, when a pre-defined water-filled gap extends to the base of the I-wall. Differences in the analyses can be anticipated as the LEM calculations were restricted to circular arc failure mechanisms (using conventional methods of slices with Spencer's method; Spencer, 1967).

Figure 6 illustrates results of the upper bound (UB) analyses (for the IPET model geometry) at a surge elevation, El. +7ft with and without the gap model. Although the extent of the failure mechanisms is comparable to the critical circular mechanisms described by Duncan et al. (2008), the UB failure mechanism with gap formation, Figs. 6a, b involve more lateral translation of the fill material, while upward rotation is only significant beyond the toe of the levee. For cases without gap formation the critical mechanisms (Figs. 6c, d) extend far below the toe of the I-wall (to El. -35ft).

There is better agreement between the current limit analyses and results of finite element analyses (using Plaxis<sup>TM</sup>; IPET, 2007). The IPET FEM analyses introduce a water-filled gap once the storm surge level in the canal reaches El. +6.5ft (based on computed tensile stress conditions). Once the gap is introduced at this elevation a FS decreases from 1.46 to 1.16. There is very good agreement between the numerical limit analyses (average of LB and UB values) and the FEM results both before and after the gap formation and the two analyses predict the same critical storm surge elevation.

Although there is a consistent agreement in the computed FS, some essential differences in the treatment of the water-filled gap should be noted here. The FEM analyses introduce the gap above a certain water level, while LEM analyses predefine the occurrence of a full-depth gap. In contrast, the numerical limit analyses allow for the possible occurrence of a water-filled gap but do not predefine it. This implies that a water-filled gap can be present at failure at any storm surge elevation with several possible states (a full-depth gap, a partial-depth gap, or non-existent). Inspection of the UB results shows that a full-depth gap always occurs at failure for water levels above El. 0ft. This demonstrates that a fully developed water-filled gap along waterside soil-wall interfaces is indeed a necessary condition for the critical failure, and the effect should be taken into account at all surge elevations (once the water rises above levee fill.). Nevertheless the effects of the gap become less significant at lower surge elevations, as indicated

by the small differences in computed FS values (with and without the gap model) below El. +5ft in Figure 5.

## EVALUATION OF THE ILIT ANALYSES

The ILIT study (ILIT, 2006; Seed et al., 2008c) includes a more detailed evaluation of the engineering geology and engineering properties of the soils at the 17<sup>th</sup> Street Canal breach site. The ILIT cross-section, Figure 1b includes several key differences in interpreted stratigraphy that can be summarized as follows:

- 1) The levee fill is sub-divided into two upper (brown) and lower (grey) clay units of different undrained shear strength (cf. Fig. 4).
- 2) The stratum boundaries are deformed beneath the levees to conform with expected consolidation-induced settlements of the levee fill.
- 3) There is an intermixing zone between the upper organic, marsh and lower lacustrine clay units. Seed et al. (2008c) report the existence of a thin (one inch in thickness) continuous layer of sensitive organic clayey silt extending from an elevation close to the toe of the I-wall. They assert that this layer has lower shear strength than the surrounding strata and corresponds to the critical translational sliding surface (Fig. 1b).

The influence of these discrepancies on the overall stability is of interest in this study, especially the role of the thin weak layer and its contribution to the breach of the 17<sup>th</sup> Street Canal I-wall.

Figure 4b presents the mesh used for lower and upper bound limit analyses of the ILIT model geometry. Table 1 summarizes the total unit weights of each layer reported by ILIT (2006). These values are comparable with those assumed by IPET except in the Lacustrine clay. The undrained shear strength properties of each stratum were extracted from the ILIT report. The profiles at several specific vertical sections are summarized in Figure 4c. The ILIT team has made a very careful interpretation of available CPTU data from the post-failure investigations. They report that the clay can be overconsolidated due to desiccation, which is significant in the clay stratum beneath the protected-side levee toe and in the free field beyond the toe. This differs from the IPET assumption that clay is normally consolidated, and also explains why the strength of clay in the ILIT model is much higher than the counterpart conditions in the IPET profile at sections D and E (Fig. 4c).

It should be noted that there are some uncertainties involved in the determination of strength properties reported by ILIT (2006). The current limit analyses assume that the shear strength of the intermixing zone is equal to that at the top of the underlying clay. In addition, some engineering judgment was needed to identify the regions of overconsolidated and normally consolidated clay.

The simulation of the thin weak layer is accomplished by placing velocity discontinuities along the layer (Fig. 1b). The shear strength distribution along the weak stratum (ILIT, 2006) is also marked on the vertical sections in Figure 4c.

Lower and upper bound limit analyses have been performed using three representations of the undrained shear strength,  $s_u$ , in the weak layer as indicated in Figure 7b:

- A) Weak layer has  $s_u$  identical to the adjacent intermixing zone (i.e., no influence of weak layer)
- B) Weak layer  $s_u$  correspond to values quoted in ILIT (2006).
- C) Weak layer  $s_u$  set at 50% of values reported by ILIT (2006).

Figure 7a summarizes the computed factors of safety for the storm surge elevation varying from 5 to 9ft. They are compared with the ILIT LEM solutions<sup>5</sup> for cases where a full-depth gap is assumed along the canal side of the I-wall and for cases with and without the presence of the weak layer.

There is relatively good agreement between FS values computed by the current numerical limit analyses and LEM results presented by ILIT (2006) for Case A (no weak layer). The LEM results are close to LB values at each of the 5 surge elevations considered and discrepancies are attributable to uncertainties in the interpretation of undrained shear strengths for the ILIT model. ILIT (2006) reports large changes in FS when the weak layer is introduced into the LEM analyses. This is not consistent with the current numerical limit analyses. Case B calculations show a relatively small reduction in undrained stability and do not match the ILIT LEM results. In fact the undrained shear strength of the weak layer has to be reduced by 50% (Case C) in

---

<sup>5</sup>There are no direct comparisons with ILIT FEM analyses as the latter use the Plaxis<sup>TM</sup> 'soft soil' constitutive model in which undrained shear strengths depend on the consolidation effective stress state prior to storm loading. These values are not explicitly stated in the published reports. ILIT find close agreement between FEM and LEM analyses.

order to approach the ILIT results. These results suggest potential errors or discrepancies in either the reported ILIT shear strength parameters or LEM analyses.

The numerical limit analyses suggest that the influence of the weak layer may not be as significant as reported by ILIT (2006). Given the limited evidence available to prove the existence of a continuous weak layer, it does not appear necessary to explain the breach of the 17<sup>th</sup> Street Canal I-wall.

Figure 8 compares numerical limit analyses (with the gap model) for the factor of safety for Case A ILIT and IPET models. These results show that higher FS values are predicted for the Case A ILIT model. This is consistent with differences in the general stratigraphy and undrained shear strength profiles considered in the two studies (cf. Figs. 1 and 4). The analyses for ILIT Case A suggest the failure of I-wall would occur at a surge elevation El. +10.5±0.5ft while the IPET model results predict failure at El. +8.5±1.0ft.

Figure 9 presents the UB failure mechanisms for the IPET (Figs. 9a, b) and ILIT Case A (Figs. 9c, d) models. Both cases predict the occurrence of full-depth, water-filled gaps and show large lateral translation mechanisms for the levee fill. The failure surface for the IPET model extends through the top of the normally consolidated lacustrine clay layer, whereas the ILIT Case A produces a mechanism that occurs within the marsh and intermixing zones (cf. Fig. 4c).

The IPET study (IPET, Vol. IV, 2007) provides a detailed assessment of the storm surge conditions during Hurricane Katrina and timing of the breach at the 17<sup>th</sup> Street Canal based on limited hydrograph gage data and various eyewitness sources. The reconstructed hydrograph at the outlet of the 17<sup>th</sup> Street Canal shows the storm surge rising from El. +7ft at 0600hrs on August 29, 2005 to a maximum surge at El. +10.5ft at around 0900hrs. The breach may have occurred somewhat earlier than the peak surge event. Based on this data, the IPET and ILIT Case A models both provide credible estimates of the critical surge elevation. However, from a geotechnical perspective, ILIT Case A includes a more realistic representation of the sub-surface stratigraphy, geology and engineering properties and hence, contributes a refined prediction of the critical surge height and failure mechanism.

## CONCLUSIONS

Numerical limit analyses have been successfully applied to evaluate the undrained stability of the 17<sup>th</sup> Street Canal I-wall levee during Hurricane Katrina. The effects of a water-filled gap

along the canal-side soil-wall interface are modeled in the proposed lower and upper bound formulations (Sloan & Kleeman, 1995; Sloan, 1988a; Ukritchon et al., 1998 and 2003), by modifying the yield surface and introducing associated energy terms, respectively. Using the proposed gap model it has been found that a water-filled gap extending along the full depth of the soil-wall interface is a necessary condition for the critical failure and can occur at all storm surge elevations.

The Authors have reproduced the cross-section geometries, sub-surface stratigraphies and engineering properties at the critical section of the I-wall as reported in forensic studies by IPET (2007) and ILIT (2006). The numerical limit analyses are in close agreement with safety factors (FS) computed by finite element (FEM with  $c$ - $\phi$  reduction) and limit equilibrium (LEM) stability analyses reported for the IPET model (IPET, 2007; Duncan et al., 2008). The UB limit analyses describe more realistic translational failure mechanisms (compared to circular arc surfaces reported by Duncan et al., 2008) and require no a priori judgment on the occurrence of the water-filled gap.

Similar comparisons have been made with LEM analyses reported by ILIT (2006). The numerical limit analyses are consistent with predictions for ILIT Case A (no weak organic clay layer), and suggest potential errors in the reported undrained shear strength or stability analyses when a weak organic clay layer is introduced in the model (Case B). The ILIT Case A model provides a more credible geotechnical representation of the sub-surface stratigraphy and engineering properties. Numerical limit analyses of ILIT Case A offer the more credible estimates for the critical surge height (El. +10.5f±0.5ft) and failure mechanism for the 17<sup>th</sup> Street Canal I-wall.

## ACKNOWLEDGMENTS

The second author (AJW) served as a member of the NRC Committee on New Orleans Regional Hurricane Protection Projects, and was closely involved in reviewing geotechnical aspects of the work conducted by IPET. The first Author (YY) has been partially supported by the National Research Foundation of Singapore and the Singapore-MIT Alliance for Research and Technology (SMART) through the Center for Environmental Modeling and Sensing (CENSAM).

## REFERENCES

- Bolton, M.D. and Powrie, W. (1987). "The collapse of diaphragm walls retaining clay." *Géotechnique*, 37(3), 335-353.
- Brinkgreve, R. (2007). *PLAXIS 2D. Version 8.5 finite-element code for soil and rock analyses: Complete set of manuals*, R. Brinkgreve, ed., Balkema, Rotterdam, The Netherlands.
- Brinkgreve, R.B.J., and Bakker, H.L. (1991). "Non-linear finite element analysis of safety factors." *In Proceedings of the 7th International Conference on Computational Methods and Advances in Geomechanics, Cairns, Australia, 6–10 May 1991. A.A. Balkema, Rotterdam, the Netherlands.* 1117–1122.
- Duncan, J.M., Brandon, T.L., Wright, S.G., and Vroman, N. (2008). "Stability of I-walls in New Orleans during Hurricane Katrina." *ASCE Journal of Geotechnical and Geoenvironmental Engineering*, 134(5), 681–691.
- Independent Levee Investigation Team (ILIT). (2006). "Investigation of the performance of the New Orleans regional flood protection systems during Hurricane Katrina." *Final Rep.*, <[http://www.ce.berkeley.edu/new\\_orleans/](http://www.ce.berkeley.edu/new_orleans/)>(July 31, 2006).
- Interagency Performance Evaluation Task Force (IPET). (2007). "Performance evaluation of the New Orleans and southeast Louisiana hurricane protection system." *Final Rep. of the Interagency Performance Evaluation Task Force, U.S. Army Corps of Engineers*, <<https://ipet.wes.army.mil>>.
- Krahn, J. (2004). *SLOPE/W: Complete Set of Manuals*, J. Krahn, ed., Calgary, Alta., Canada.
- Ladd, C.C. (2009). "Discussion of 'Stability of I-walls in New Orleans during Hurricane Katrina' by Duncan et al." *ASCE Journal of Geotechnical and Geoenvironmental Engineering*, 135(12), 1999-2002.
- Lambe, T.W. and Whitman, R.V. (1969). *Soil Mechanics*. John Wiley and Sons, Inc., New York.
- Sasanakul, I., Vanadit-Ellis, W., Sharp, M. K., Abdoun, T. H., Ubilla, J. O., Steedman, R. S., and Stone, K. J. L. (2008). "New Orleans levee system performance during Hurricane Katrina: 17th Street Canal and Orleans Canal North," *ASCE Journal of Geotechnical and Geoenvironmental Engineering*, 134(5), 657–667.
- Seed, R. B., Bea, R. G., Athanasopoulos-Zekkos, A., Boutwell, G. P., Bray, J. D., Cheung, C., Cobos-Roa, D., Harder, L. F., Moss, R. E. S., Pestana, J. M., Porter, J., Riemer, M. F., Rogers, J. D., Storesund, R., Vera-Grunauer, X., and Wartman, J. (2008c). "New Orleans

- and Hurricane Katrina. III: The 17th Street drainage canal.” *ASCE Journal of Geotechnical and Geoenvironmental Engineering*, 134(5), 740–761.
- Sloan, S.W. (1988a). “Lower bound limit analysis using finite elements and linear programming.” *Int. J. Numer. Anal. Methods in Geomech.* 12(1), 61-77.
- Sloan, S.W. (1988b). “A steepest edge active set algorithm for solving sparse linear programming problems.” *Int. J. Numer. Anal. Methods. In Geomech.* 26(12), 2671-2685.
- Sloan, S.W., and Kleeman, P.W. (1995). “Upper bound limit analysis using discontinuous velocity fields.” *Comp. Methods in Appl. Mech. And Engrg.*, 127, 293-314.
- Spencer, E. (1967) “A method of analysis of the stability of embankments assuming parallel interslice forces.” *Géotechnique*, 17(1), 11-26.
- Ukritchon, B., Whittle, A.J., and Sloan, S.W. (1998). “Undrained limit analyses for combined loading of strip footing on clay.” *ASCE Journal of Geotechnical and Geoenvironmental Engineering*, 124(3), 265-276.
- Ukritchon, B., Whittle, A.J., and Sloan, S.W. (2003). “Undrained stability of braced excavations in clay.” *ASCE Journal of Geotechnical and Geoenvironmental Engineering*, 129(8), 738-754.
- Wright, S.G. (1999). *UTEXAS4—A computer program for slope stability calculations*, Shinoak Software, Austin, Tex.



## APPENDIX. NOTATION

*The following symbols are used in this paper:*

- $F_x, F_y, F_z$  = force components for joint elements;
- $p_w$  = hydrostatic water pressure;
- $s_u$  = undrained shear strength of clay;
- $u, v$  = velocity components in x,y direction, respectively;
- $w$  = angular velocity for joint elements;
- $W_{bm}$  = plastic power dissipation in beam elements;
- $W_{dis}$  = plastic power dissipation in velocity discontinuities and soil-structure interfaces;
- $W_{ele}$  = plastic power dissipation in soil elements;
- $W_{ext}$  = total external rate of work;
- $W_g$  = external rate of work done by gravity force;
- $W_{gap}$  = external rate of work due to the formation of water-filled gap;
- $W_{hyd}$  = external rate of work done by hydraulic pressure;
- $W_{int}$  = total internal power dissipation;
- $\Delta u_n$  = normal velocity jump across soil-structure interfaces;
- $\sigma_n, \tau$  = normal and shear stress across soil-structure interfaces;
- $\sigma_x, \sigma_y, \tau_{xy}$  = stress components in plane strain soil elements;
- $\tau_m$  = mobilized shear stress in stability calculation;

**Table 1.** Total unit weight of each layer in the IPET and the ILIT model

	Layer	$\gamma_t$ [pcf]
<b>IPET</b>	Fill	110
	Marsh	80
	Lacustrine clay	109*
<b>ILIT</b>	Upper fill	110
	Lower fill	85
	Marsh	80
	Weak layer	80
	Intermixing zone	90
	Lacustrine clay	90*

\*Ladd (2008) suggests the mean values of the total unit weight of the Lacustrine clay are 102.4 pcf beneath the levee crest and 97.5 pcf beneath the toe.

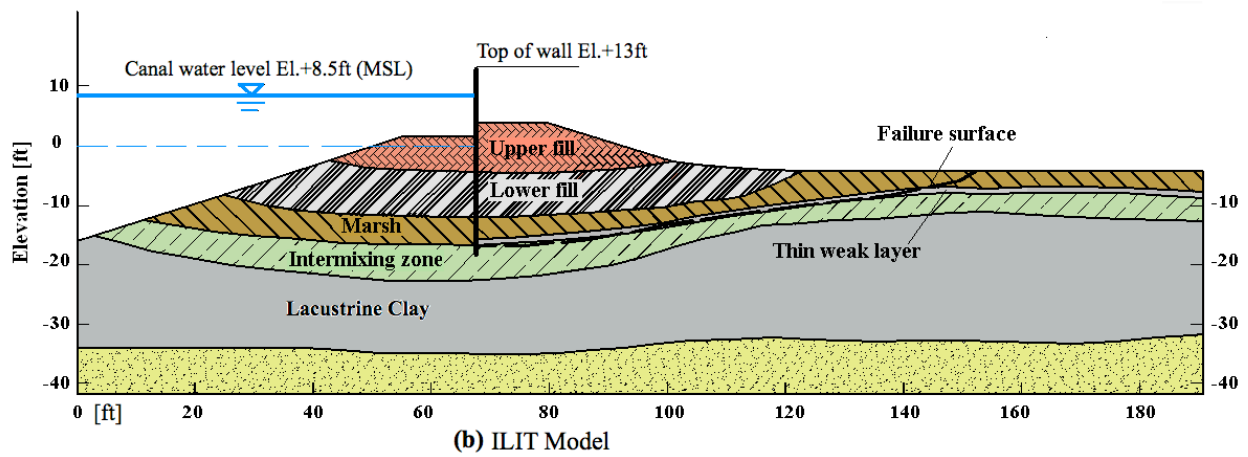
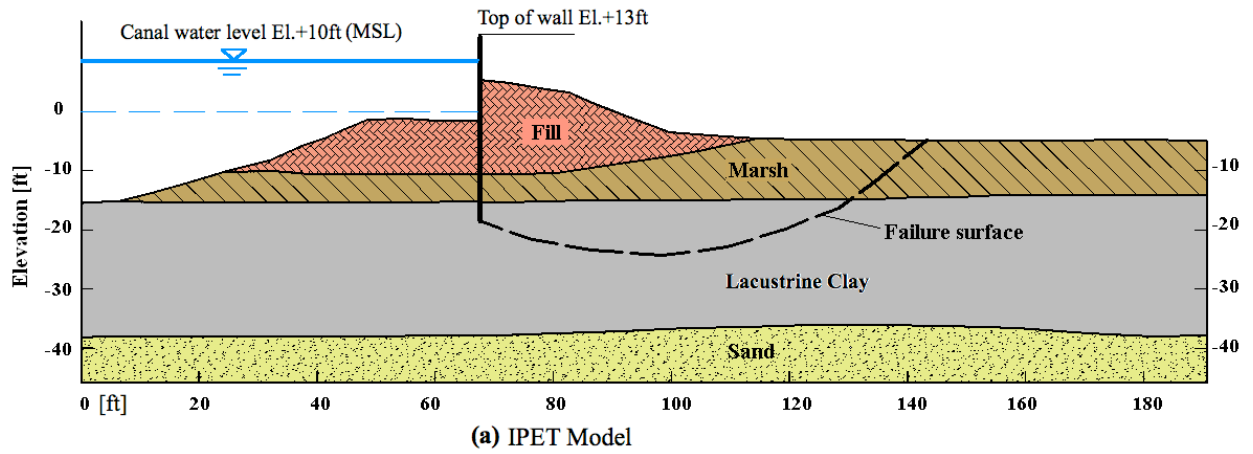


**Figure 1.** (a) IPET and (b) ILIT interpreted cross-section and proposed failure mechanisms (Duncan et al., 2008; Seed et al., 2008)

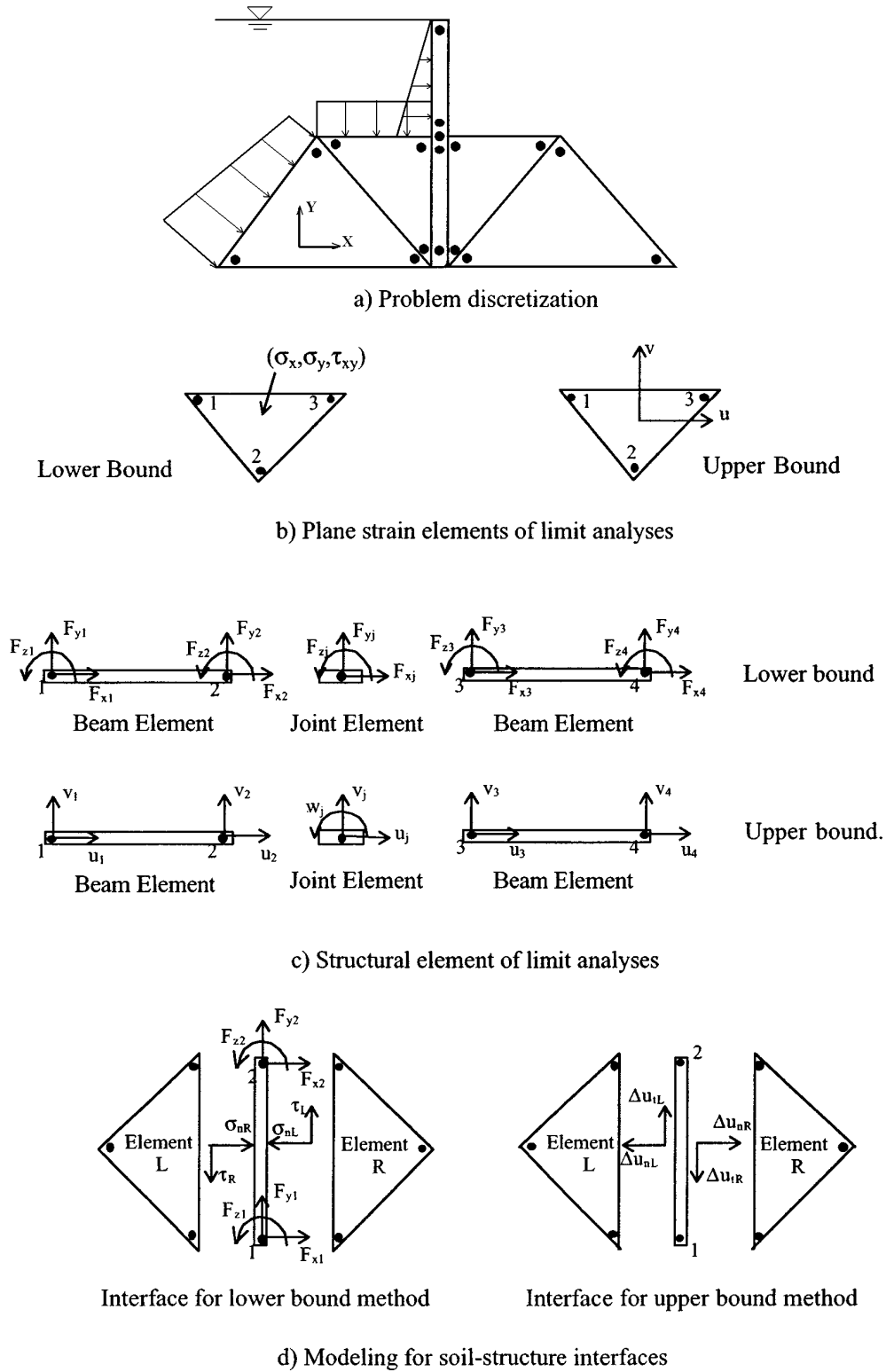


**Figure 2.** Problem discretization for levee stability and summary of plane-strain elements in numerical limit analyses (after Ukritchon et al., 2003)

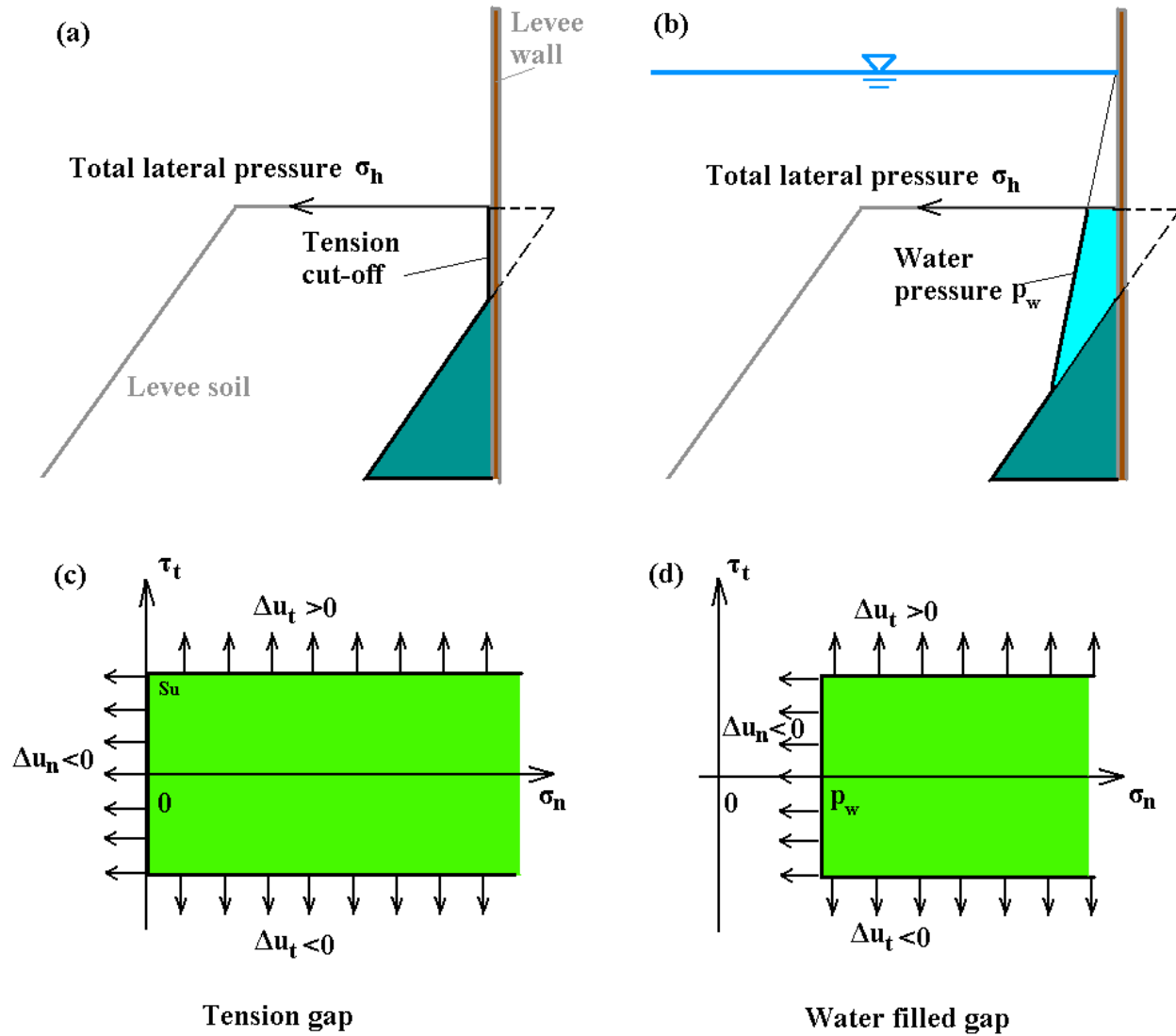


**Figure 3.** Flow rule associated with modified Tresca yield criterion for (a) tension gap and (b) water-filled gap; Admissible lateral stress profile along soil-wall interface to account for (c) tension gap and (d) water-filled gap

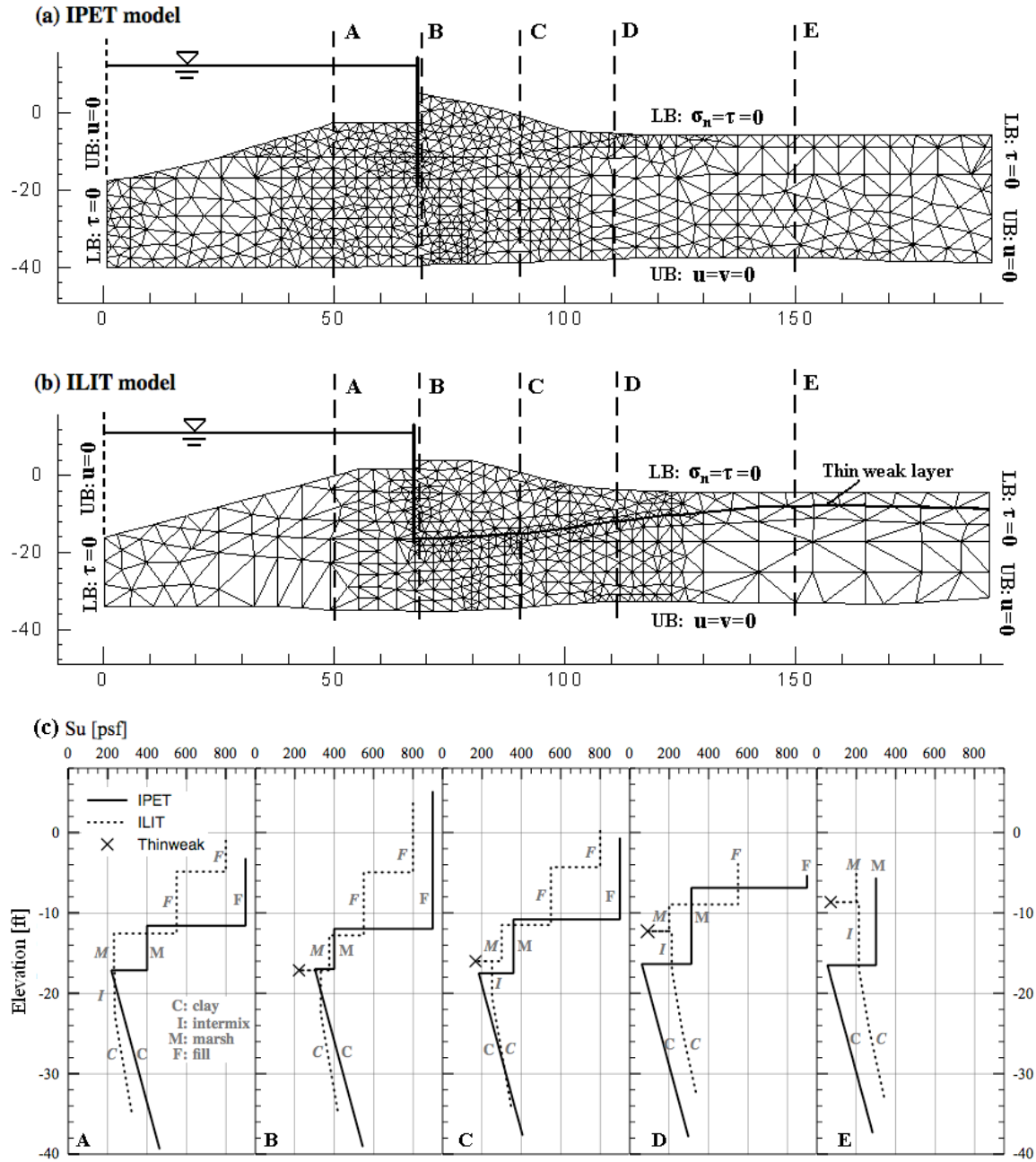


**Figure 4.** (a) The IPET model mesh; (b) the ILIT model mesh and (c) undrained shear strength profiles used in numerical limit analyses of 17<sup>th</sup> Street Canal I-wall levee stability

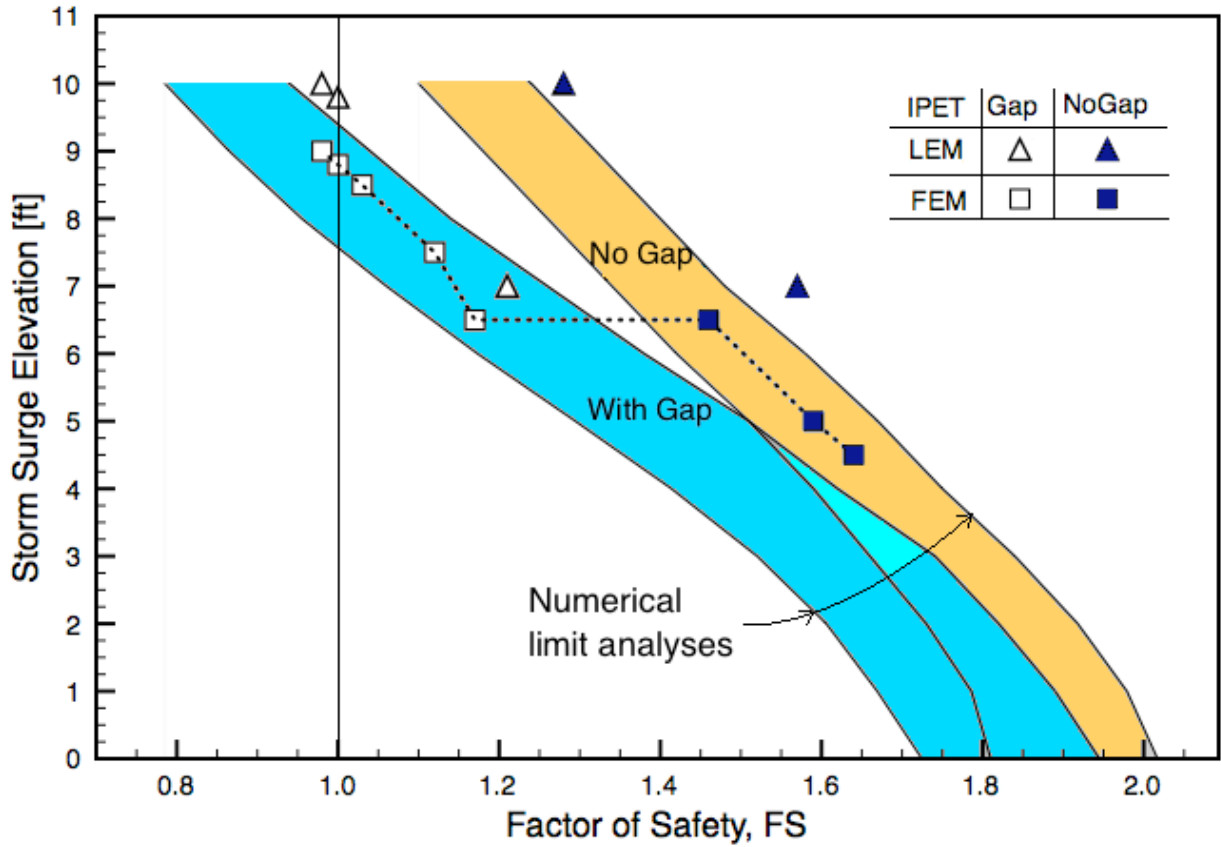
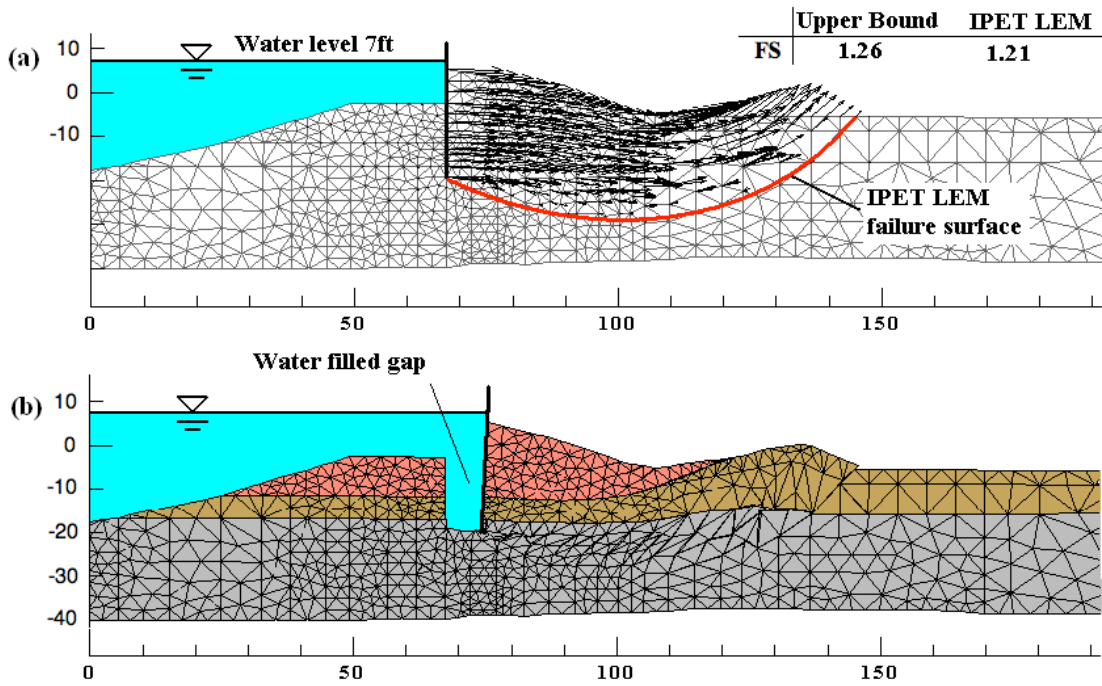


**Figure 5.** Comparison of I-wall stability using FS of numerical limit analyses with results of analyses reported by IPET

**With gap**



**No gap**

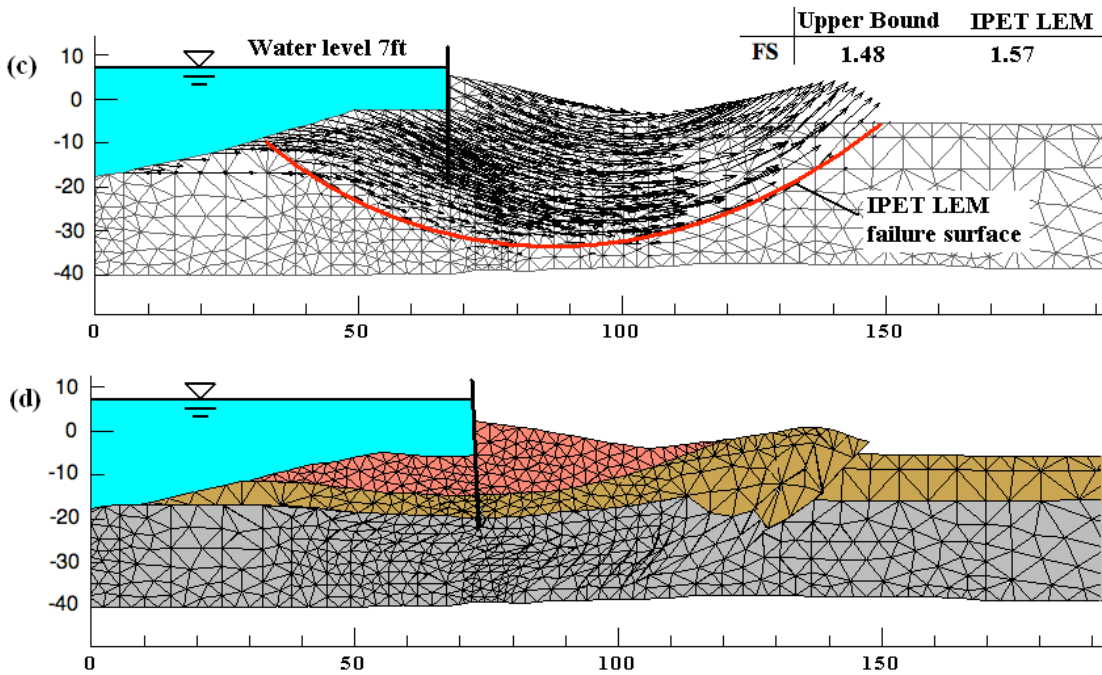


**Figure 6.** Results of upper bound analyses for the IPET model at a surge elevation, El.+7ft



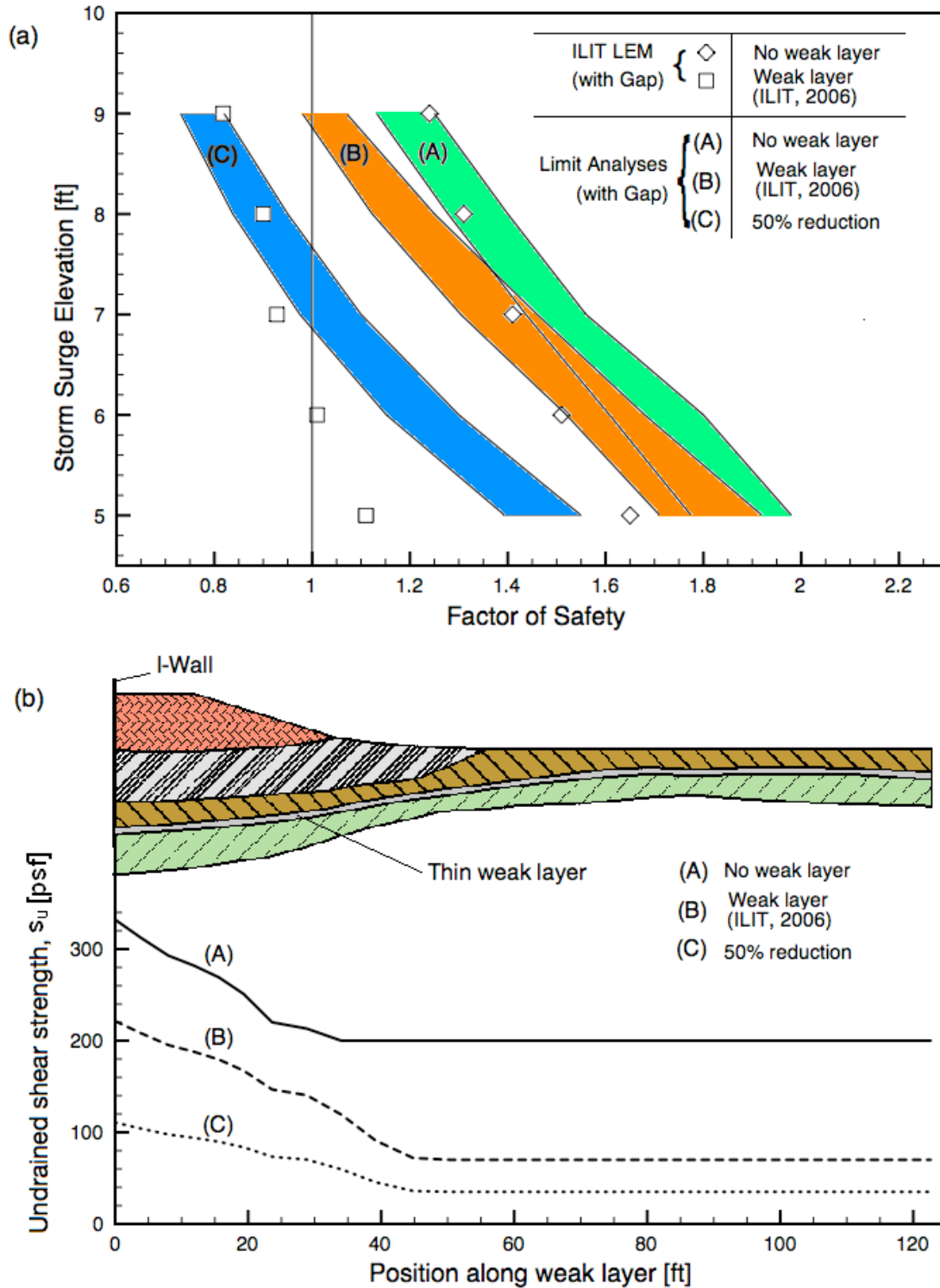


**Figure 7.** (a) Comparison of factor of safety between numerical limit analyses and the ILIT LEM analyses; (b) Undrained shear strength along the thin weak layer

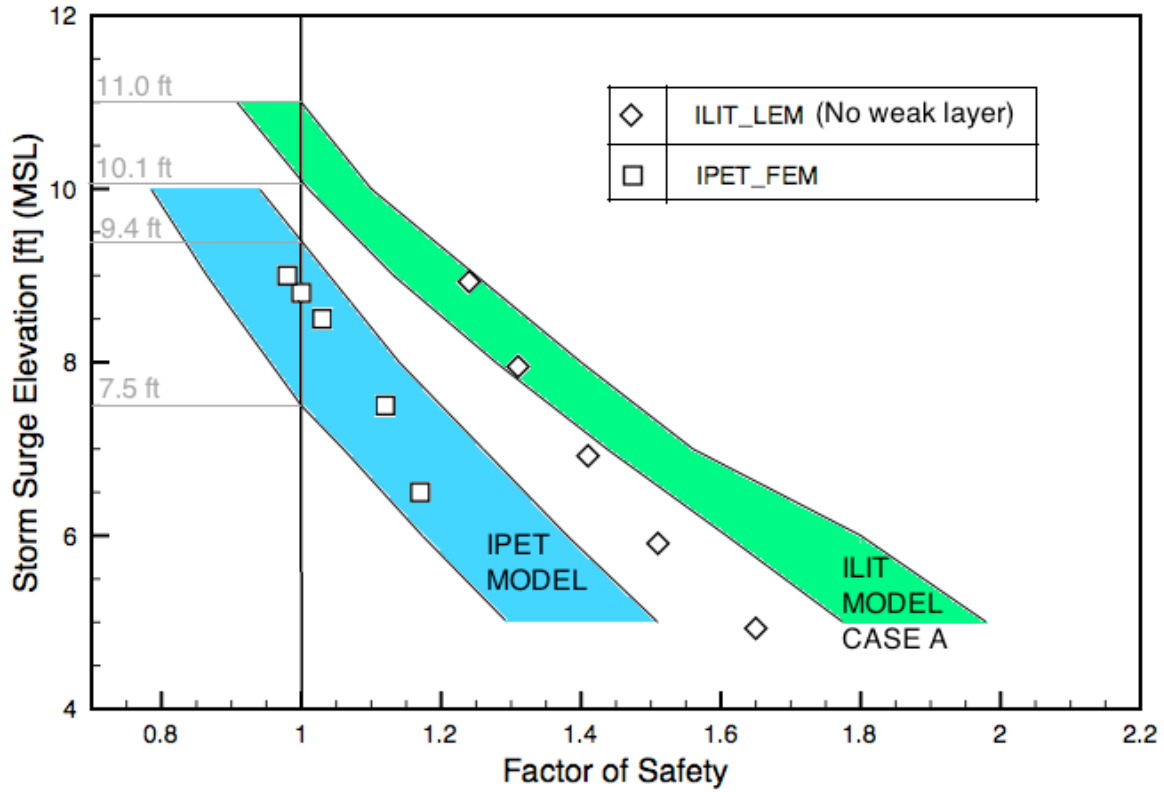
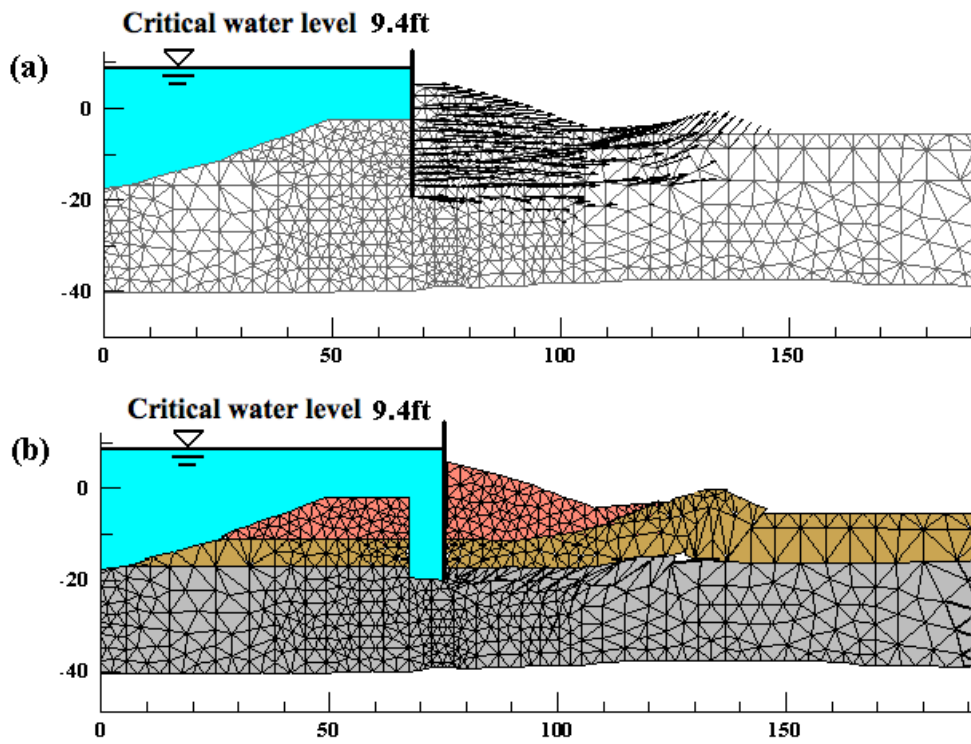


**Figure 8.** Factor of safety of numerical limit analyses using both the IPET and ILIT Case A model with full depth water-filled gap.

## IPET model



## ILIT Case A model

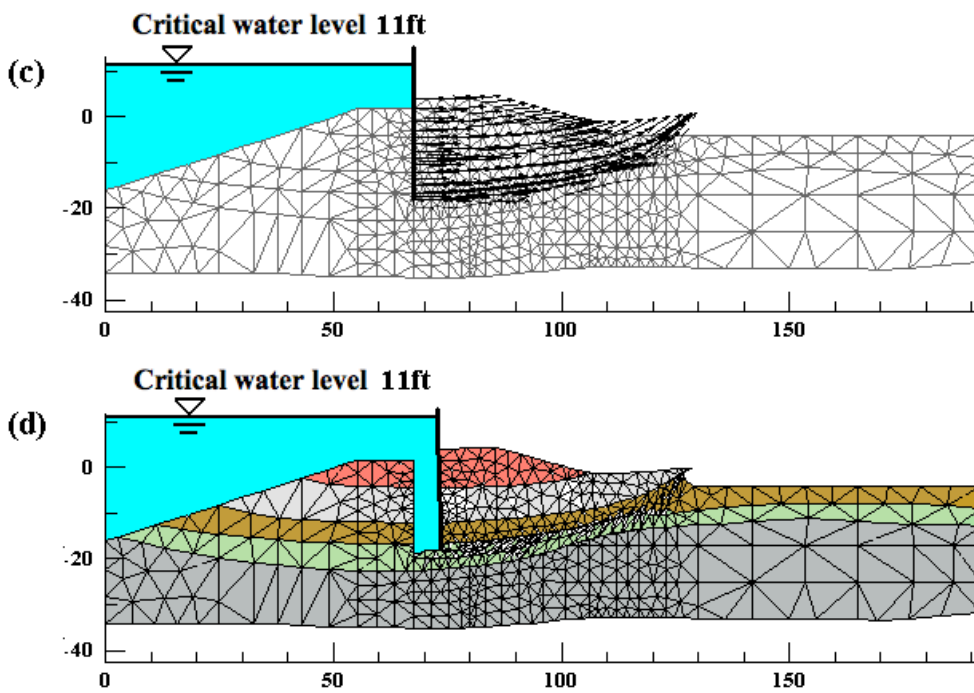


**Figure 9.** UB failure mechanisms obtained using the IPET and ILIT Case A models at each critical surge elevation